Physics

Electricity & Magnetism fields

Okayama University $\qquad$ *Year* 1985

Finite element analysis of magnetic fields taking into account hysteresis characteristics

Takayoshi Nakata
Okayama University

N. Takahashi
Okayama University

Y. Kawase
Okayama University

FINITE ELEMENT ANALYSIS OF MAGNETIC FIELDS
TAKING INTO ACCOUNT HYSTERESIS CHARACTERISTICS

T. Nakata, N. Takahashi and Y. Kawase

ABSTRACT

A new technique for taking into account hysteresis has been developed.

The paper describes the details of the method and the usefulness of the technique is clarified by applying it to the analysis of magnetic fields in single-phase transformer cores. The calculated results are in good agreement with the measured ones.

1. INTRODUCTION

Hysteresis characteristics of the core should be taken into account in order to calculate accurately the flux waveform at each point in the core. When reluctivity is used in the calculation, analysis becomes difficult because the reluctivity corresponding to the hysteresis loop is not continuous when the flux density is equal to zero[1,2].

In this paper, a new technique for taking into account hysteresis is discribed, which avoids this difficulty. The effects of hysteresis on the flux distributions and the flux waveforms in a transformer core are investigated using the new method.

2. METHOD OF ANALYSIS

2.1 Fundamental equations

In the finite element analysis of magnetic fields, a Poisson's equation, which is a function of magnetic vector potential and reluctivity, is solved[1]. The reluctivity can represent the hysteresis loop shown in Fig.1(a), but it becomes infinite at the points α_1 and α_2, where the flux densities B are equal to zero as shown in Fig.1(b). Thus, the representation of the hysteresis loop is difficult using the reluctivity ν. Alternately, if the hysteresis loop is represented by the magnetization $\mathbf{M}$, and the relationship among $\mathbf{B}$, $\mathbf{M}$ and the intensity of the magnetic field $\mathbf{H}$, is denoted by the following equation, the difficulty is avoided because the M-B curve becomes a continuous one as shown in Fig.1(c).

$$\mathbf{B} = \mu_0\mathbf{H} + \mathbf{M} \tag{1}$$

Where μ_0 is the permeability of air.

By applying the Ampere's circuital law to Eq.(1), the following equation is obtained:

$$\mathrm{rot}\,\frac{1}{\mu_0}(\mathbf{B} - \mathbf{M}) = \mathbf{J}_0 \tag{2}$$

Where $\mathbf{J}_0$ denotes the current density. Eq.(2) may be rewritten as

$$\nu_0\,\mathrm{rot}\,\mathrm{rot}\,A = \mathbf{J}_0 + \mathbf{Jm} \tag{3}$$

Where A is the magnetic vector potential. $\mathbf{Jm}$ is the equivalent magnetizing current density and is expressed by

$$\mathbf{Jm} = \nu_0\,\mathrm{rot}\,\mathbf{M} \tag{4}$$

In a two-dimensional analysis, Eqs.(3) and (4) may be written as

---

The authors are with the Department of Electrical Engineering, Okayama University, Okayama 700, Japan.

(a) hysteresis loop   (b) ν-B curve

(c) M-B curve

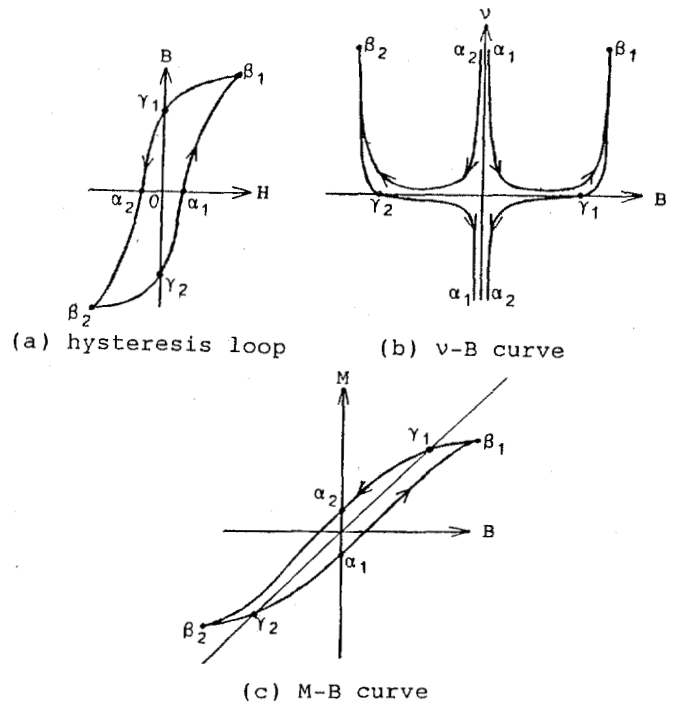Fig.1 Various representations of magnetic hysteresis.

$$\nu_0\left(\frac{\partial^2 A}{\partial x^2} + \frac{\partial^2 A}{\partial y^2}\right) + \mathbf{J}_0 + \mathbf{Jm} = 0 \tag{5}$$

$$\mathbf{Jm} = \nu_0\left(\frac{\partial My}{\partial x} - \frac{\partial Mx}{\partial y}\right) \tag{6}$$

where A, Jo and Jm are the z-directional components of A, $\mathbf{J}_0$ and $\mathbf{Jm}$ respectively. Mx and My are the x- and y-directional components of $\mathbf{M}$.

2.2 Finite element formulation

The following equation can be obtained by the Galerkin method from Eqs.(5) and (6) [3].

$$
\begin{aligned}
Gi = \sum_{e=1}^{NE}\Bigg\{ &\iint_{S^{(e)}} \sum_{k=1}^{3} \nu_0\left(\frac{\partial Ni^{(e)}}{\partial x}\cdot\frac{\partial Nke}{\partial x} + \frac{\partial Ni^{(e)}}{\partial y}\cdot\frac{\partial Nke}{\partial y}\right)Ake\,dx\,dy \\
&-\iint_{S^{(e)}} Ni^{(e)} Jo\,dx\,dy \\
&-\iint_{S^{(e)}} \nu_0\left(Mx\frac{\partial Ni^{(e)}}{\partial y} - My\frac{\partial Ni^{(e)}}{\partial x}\right)dx\,dy \Bigg\} = 0
\end{aligned}
\tag{7}
$$

Where NE is the number of elements, and $Ni^{(e)}$ is the interpolation function of an element e [3]. Ake is the vector potential of a node ke.

By expanding Gi in a multidimensional Taylor's series in increments of δAi, the following matrix equation for the Newton-Raphson iteration scheme is obtained [3]:

$$\begin{bmatrix} \dfrac{\partial G_1}{\partial A_1} \cdots\cdots\cdots \dfrac{\partial G_1}{\partial A_n} \\ \dfrac{\partial G_i}{\partial A_j} \\ \dfrac{\partial G_n}{\partial A_1} \cdots\cdots\cdots \dfrac{\partial G_n}{\partial A_n} \end{bmatrix} \begin{Bmatrix} \delta A_1 \\ \vdots \\ \delta A_i \\ \vdots \\ \delta A_n \end{Bmatrix} = \begin{Bmatrix} -G_1 \\ \vdots \\ -G_i \\ \vdots \\ -G_n \end{Bmatrix} \qquad (8)$$

where n is the number of nodes of which the vector potentials are unknown. $G_i^{(e)}$ of an element e is calculated from Eq.(7) as follows:

$$G_i^{(e)} = \nu_0 \sum_{k=1}^{3} S_{ike} A_{ke} - \frac{\Delta^{(e)}}{3} J_o^{(e)} - \frac{\nu_0}{2}(M_x^{(e)} d_i^{(e)} - M_y^{(e)} c_i^{(e)}) \qquad (9)$$

Where Sike is defined by

$$S_{ike} = \frac{1}{4\Delta^{(e)}}(c_i^{(e)} c_{ke} + d_i^{(e)} d_{ke}) \qquad (10)$$

$\Delta^{(e)}$ is the area of the element e, and c_{ie} and d_{ie} are denoted by

$$\left.\begin{matrix} c_{ie} = y_{je} - y_{ke} \\ d_{ie} = x_{ke} - x_{je} \end{matrix}\right\} \qquad (11)$$

with the other coefficients obtained by a cyclic permutation of subscripts in the order i, j, k. $\partial G_i^{(e)}/\partial A_j$ can be derived from Eq.(9) as follows:

$$\frac{\partial G_i^{(e)}}{\partial A_j} = \nu_0 S_{ij}^{(e)}$$
$$- \frac{\nu_0}{4\Delta^{(e)}}(\frac{\partial M_x^{(e)}}{\partial B_x^{(e)}} \cdot d_i^{(e)} \cdot d_j^{(e)} + \frac{\partial M_y^{(e)}}{\partial B_y^{(e)}} \cdot c_i^{(e)} \cdot c_j^{(e)})$$
$$\qquad (12)$$

In Eq.(12), Mx and My are assumed to be the functions of the x- and y-components Bx and By of the flux density $\mathbb{B}$ respectively.

2.3 Process of calculation

Typical d.c. hysteresis loops are stored in a computer to represent hysteresis phenomena as shown in Fig.2. Hysteresis loop 1 with the maximum flux density Bm is interpolated from these typical hysteresis loops as shown in Fig.3. The new loop P-Q-R-S-P is obtained from two nearest typical loops 2 and 3. Two forms of the M-B curves, in the rolling and the transverse directions, are necessary to analyze the magnetic circuit when anisotropic material such as grain-oriented silicon steel is used.

The process of calculation is as follows: In the first few time steps (ωt), the flux distribution is calculated using the initial magnetization curve denoted by the chain line in Fig.3. If the flux density reaches the maximum value Bm at the point P, demagnetization progresses along the upper branch a' of
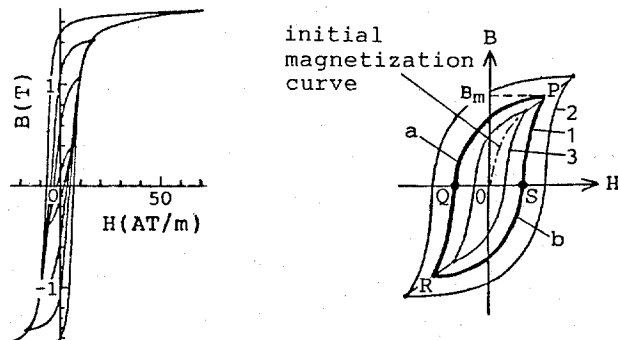
the hysteresis loop. When the demagnetization reaches a state of opposite magnetization at the point R, remagnetization takes place along the lower branch b. The above-mentioned process is repeated until a steady state is reached.

3. EXAMPLES OF APPLICATION[2]

Magnetic characteristics of single-phase, transformer cores are analyzed. In these problems, hysteresis characteristics should be taken into account in order to analyze the flux waveforms accurately.

3.1 Single-phase, two-limbed core

Figure 4 shows a quarter of the analyzed single-phase, two-limbed core. The core is made of 0.3(mm) thick highly-oriented silicon steel M-OH. The hysteresis loops are shown in Fig.2. The core is excited by a sinusoidal voltage, and the overall flux density in the limb is 1.7(T).

Figure 5 shows the calculated flux distributions. Zero time is taken to be the instant when the flux density in the limb is at a maximum. Figure 6 shows the waveforms of the localized flux densities at the center of the limb. a-d correspond to the positions a-d in Fig.4. As the waveforms are not so much distorted, the calculated results of such two-limbed core is liable to agree with the results measured as shown in Fig.6.
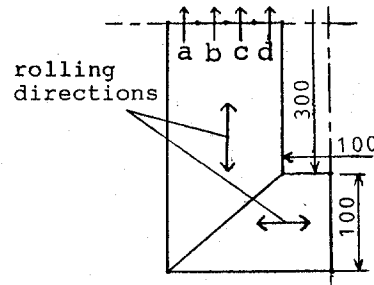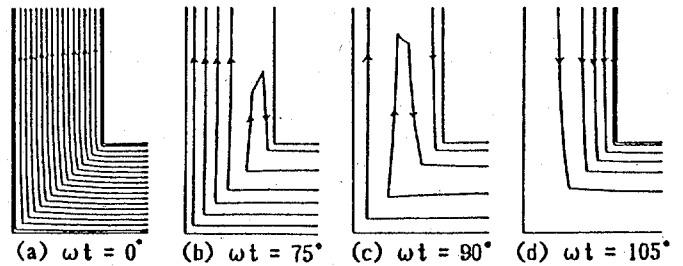
Fig.4 Single-phase, two-limbed core.

(a) $\omega t = 0°$ (b) $\omega t = 75°$ (c) $\omega t = 90°$ (d) $\omega t = 105°$

Fig.5 Flux distributions with hysteresis.

(a) calculated   (b) measured

Fig.6 Waveforms of localized flux densities.

Fig.2 Hysteresis loops for silicon steel M-OH.

Fig.3 Determination of a hysteresis loop.
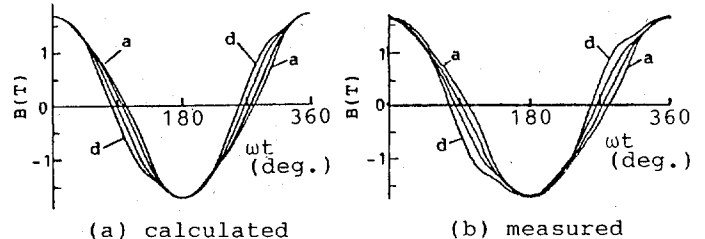
3.2 Single-phase, four-limbed core

In a single-phase, four-limbed transformer core[4] shown in Fig.7, only the inner limbs are excited, while the outer limbs are free. Therefore, the phase difference and the distortion of the flux waveforms in a four-limbed core are greater than those in a two-limbed core. The magnetic characteristics of the core, shown in Fig.7, are analyzed by taking into account hysteresis. The grade of silicon steel and the overall flux density are the same as those for the two-limbed core.

Figures 8 and 9 show the influence of hysteresis on the flux distributions. If hysteresis is neglected, the flux vanishes at $\omega t = 90°$ as shown in Fig.8(c). However, if hysteresis is taken into account, circulating fluxes exist at $\omega t = 90°$ as shown in Fig.9(c). The difference between the flux distributions at $\omega t = 75°$ and $105°$ is also caused by the hysteresis effect.

Figure 10 shows the waveforms of the localized flux densities. The waveform of each localized flux density is non-symmetric. The difference in phase angles among the localized flux densities is caused by the hysteresis effect. The calculated results with
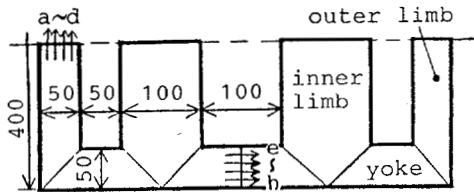

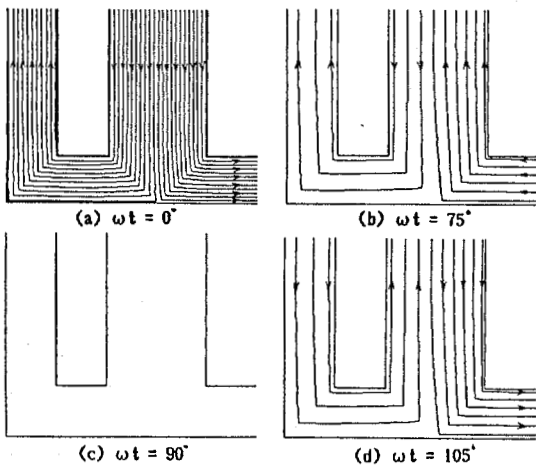Fig.7 Single-phase, four-limbed transformer core.
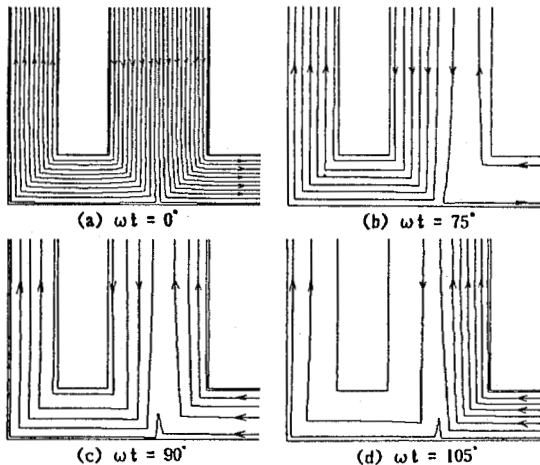

Fig.8 Flux distributions without hysteresis.

Fig.9 Flux distributions with hysteresis.

calculated results without hysteresis

calculated results with hysteresis

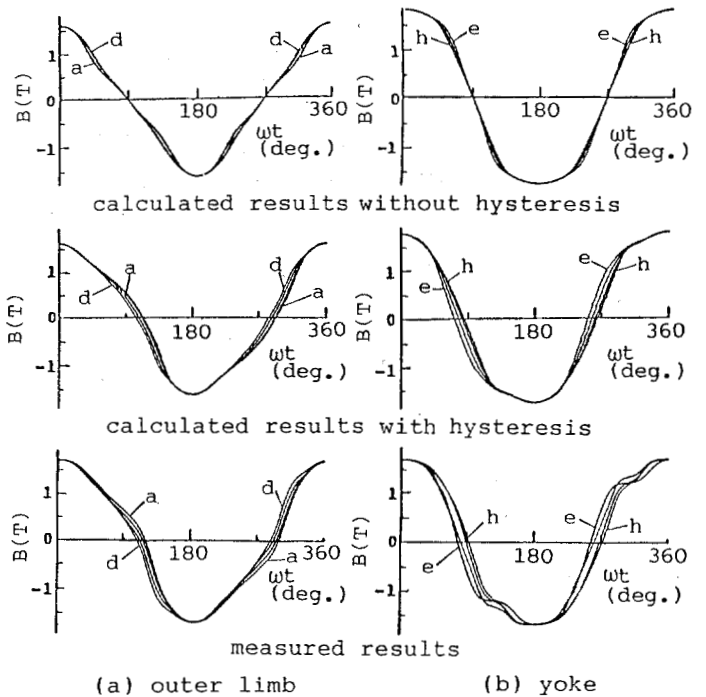measured results

(a) outer limb   (b) yoke

Fig.10 Waveforms of localized flux densities.

hysteresis shows good agreements with the results measured.

The total CPU time in the calculation with hysteresis was about 6 times as much as that without hysteresis.

4. CONCLUSIONS

By representing the magnetization characteristic of an iron core with the magnetization M, it became possible to analyze magnetic fields numerically taking into account hysteresis.

It is found that a circulating flux exists at the instant when the overall flux is zero, and that there exists phase differences among the waveforms of localized flux densities due to the hysteresis effect. If hysteresis is neglected, there are large differences in waveforms between the measured and the calculated fluxes, especially in single-phase transformer cores. Fairly accurate solutions, however, can be obtained by taking into account hysteresis.

It is hoped that this technique may be expanded to the treatment of rotational hysteresis.

REFERENCES

[1] T. Nakata, Y. Ishihara, N. Takahashi and Y. Kawase, "New Efficient Techniques for Calculating Magnetic Fields Taking into Account Hysteresis Characteristics and Eddy Currents", Papers of Technical Meeting on Information Processing, IP-80-9, IEE Japan, 1980.

[2] T. Nakata, Y. Kawase and M. Kawata, "Numerical Analysis of Flux Distributions in Transformer Cores Using the Finite Element Method Taking into Account Hysteresis Effects", Papers of Combined Technical Meeting on Rotating Machinery and Static Apparatus, RM-84-25, SA-84-9, IEE Japan, 1984.

[3] T. Nakata and N. Takahashi, "Finite Element Method in Electrical Engineering", Morikita Publishing Co., Tokyo, 1982.

[4] T. Nakata, Y. Ishihara and N. Takahashi, "Analysis on Magnetic Characteristics of Single-Phase, Four-Limbed Transformer Cores", European Physical Society Conference, Proceedings of Soft Magnetic Materials 3, 11-2, pp.351-358, 1977.